ISBN: 978-3-95450-208-0 doi:10.18429/JACoW-IPAC2019-WEPGW101

A NEW ORBIT FEEDFORWARD TABLE GENERATION METHOD FOR INSERTION DEVICES*

Y. Hidaka†, B. Kosciuk, B. Podobedov, J. Rank, T. Tanabe,
Brookhaven National Laboratory, Upton, New York, USA

Abstract

A new method of orbit feedforward (FF) table generation for insertion devices (IDs) is proposed. The main purpose of the orbit FF table is to suppress orbit disturbance around a storage ring, caused by the gap/phase motion of an ID. A conventional procedure is to measure a closed orbit at a reference ID gap/phase state, and another one at a different state, with all types of orbit feedback (FB) systems disabled. Based on the difference orbit, the correction currents for the local ID correctors are estimated to cancel the global orbit distortion. The new method instead utilizes the orbit deviation at the beam position monitors within an ID straight section (ID BPMs) with respect to a dynamically changing orbit that is defined by the orbit at two BPMs bounding the ID straight. Correction currents are determined such that this orbit deviation at the ID BPMs is minimized. Being impervious to transverse kicks external to this bounded region, this measurement can be performed with a global orbit FB system turned on, which could allow parallel table generation for multiple IDs.

INTRODUCTION

Residual first and second field integrals of an insertion device (ID) are minimized during the tuning of the device before installation to a storage ring, but cannot be corrected to a negligible level in many cases. These residual errors result in global closed orbit distortion when the state (i.e., gap or, for elliptically polarized undulators, phase) of an ID is changed. With an orbit feedback (FB) system, this distortion can be localized to the straight section where the ID is moving such that beamline experiments at other IDs are not adversely affected. However, since these ID-state-dependent orbit errors are predictable and reproducible, an orbit feedforward (FF) system is typically utilized to offload the burden on the global orbit FB (e.g., [1]).

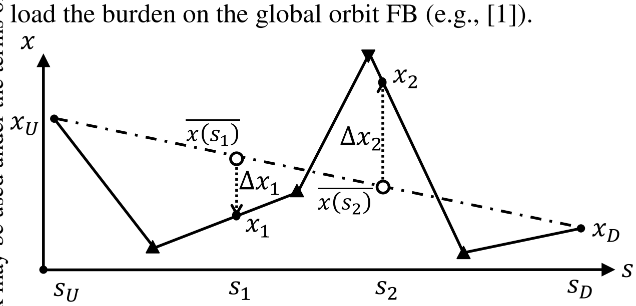

Figure 1: Schematic for dynamic orbit definitions in a region bounded by two BPMs. Triangles indicate kicks, while circles represent BPMs.

A conventional procedure involves a measurement of closed orbit at many beam position monitors (BPMs) around the ring with an ID fully open, and another measurement with the ID closed to a certain gap/phase, while any type of orbit FB is disengaged. Then the correction currents for the orbit correctors near the ID are computed to minimize the observed orbit difference. Given this procedure, it is obvious that FF table generation can be done 1) only one ID at a time and 2) only during dedicated beam studies, not user operation periods that require the use of orbit FB systems. Long-term drifts of the ID field errors also necessitate occasional table updates. Therefore, it is desirable to speed up the procedure. Depending on the types of IDs, the generation and validation of an orbit FF table can take a few tens of minutes to hours (2-D tables for EPUs), fundamentally limited by the speed at which IDs can be moved. The new method proposed in this paper can drastically reduce the total time required for generating/updating the orbit FF tables for all the IDs installed in a storage ring via parallelization.

DEFINITIONS OF DYNAMIC ORBITS

For the new FF table generation method, we use a special orbit whose reference dynamically changes. We consider a region of a storage ring bounded by two BPMs (called as bounding BPMs) located at s_U and s_D, where there are several BPMs in-between them, as shown in Fig. 1. We assume this bounded region (BR) to be an ID straight section and refer to the BPMs internal to this region (located at s_1 and s_2) as ID BPMs, for ease of understanding and connection to the new FF method we will discuss later, even though the orbit definitions do not require such an assumption. Using the raw BPM position values (i.e., values that would be normally used for orbit display and correction) x_U and x_D at the bounding BPMs, the dynamic straight-line orbit at the ID BPMs is defined as:

$$\overline{x(s_i)} \equiv \overline{x_i} \equiv \frac{x_D - x_U}{s_D - s_U}(s_i - s_U) + x_U.$$

Then the dynamically-bounded orbit (DBO) is defined as:

$$\Delta x(s_i) \equiv \Delta x_i \equiv x_i - \overline{x_i}, \tag{1}$$

where x_i is the raw BPM position at an ID BPM located at s_i within BR. Note that $\Delta x(s_U) = \Delta x(s_D) = 0$. Any one DBO can be selected as a static reference orbit $\Delta x_R(s_i) \equiv \Delta x_{Ri}$. Finally, we can define a reference-subtracted dynamically-bounded orbit (RSDBO) as follows:

$$\delta x(s_i) \equiv \delta x_i \equiv \Delta x_i - \Delta x_{Ri}. \tag{2}$$

The most important characteristic of DBO and RSDBO is that they are impervious to any transverse kick changes outside of BR that generate global orbit distortion. As long as there is no change in transverse kicks within BR, DBO

* Work supported by U.S. DOE under Contract No. DE-SC0012704.
† yhidaka@bnl.gov

ISBN: 978-3-95450-208-0 doi:10.18429/JACoW-IPAC2019-WEPGW101

will stay constant (zero in the case of RSDBO). In other words, any change in Δx_i or δx_i must come from changes in kicks only within BR. This fact, which was first realized by us during the investigation of the mysterious orbit drift problem at NSLS-II [2], is very simple, but quite powerful because RSDBO can be used to estimate an orbit FF table with a global orbit FB system turned on.

Note that the condition of no transverse kick change within BR under global orbit distortion means that BR can only contain transverse-position-independent kick elements, i.e., only drifts and time-independent dipoles.

NEW METHOD

At least two correctors for each horizontal and vertical plane are required for the primary purpose of the orbit FF system, i.e., to eliminate the global orbit distortion caused by a change in the residual field integrals when the state of an ID is changed. A global orbit FB system can be either turned on or off. After all the IDs in the straight section of interest are fully opened, a DBO is measured and designated as Δx_{Ri}. First, a response matrix $M_{i,j} \equiv d(\delta x_i)/dI_j$ needs to be measured by varying the currents of the ID correctors that will be used for the FF system. Then we close the ID to different gaps/phases, while measuring δx_i at each state, resulting in

$$\delta x_i = M \cdot \Delta I, \tag{3}$$

from which the correction currents ΔI for each state can be computed via singular value decomposition. Finally, an FF table is constructed by combining all the 1-D arrays of ΔI for each ID state. Note that you can measure both M and δx_i for multiple IDs in different straights simultaneously, because δx_i at each ID straight is isolated from each other.

EXPERIMENTAL RESULTS

A proof-of-principle experiment for the new FF table generation method was conducted at NSLS-II Storage Ring. At NSLS-II, each straight section (6.6 or 9.3 m) is bounded by 2 regular BPMs called P6 and P1. Between those bounding BPMs, there are 2 to 4 ID BPMs denoted by P7 through P10. There is also a sextupole and a fast corrector ~9 cm and ~0.7 m away from each bounding BPM.

Figure 2 demonstrates the stability of DBO. Fast Acquisition (FA) BPM data at the 10-kHz sampling rate were recorded for 10 seconds with 20 mA beam current in 1000 buckets, while all the magnet setpoints were fixed. The fast orbit feedback (FOFB) was turned off during this measurement. RMS DBO noise is reduced by a factor of up to 10 horizontally and 6 vertically (not shown), compared to raw orbit noise. This reduction largely comes from the fact that the effects of random kicks external to each BR are excluded in DBO. The residual is believed to be mainly attributed to the BPM electronic noise. Note that if one looks at FA raw orbit, rather than DBO, the FOFB typically suppresses rms noise in the bandwidth by a factor of 2-4.

As expected, the stability of DBO without FOFB was comparable to that with FOFB, as shown in Fig. 3. Theoretically there cannot be any kick sources that vary in time in BR to have stable DBO. This means that the 2 fast correctors within each BR at NSLS-II must be disabled from the FOFB loop. However, there was not much difference in terms of stability whether to keep those fast correctors enabled or disabled, as the green and red curves in Fig. 3 illustrate. This can be explained by the relationship between a transverse kick change within BR and its effect on RSDBO depicted in Fig. 4. From a simple geometry, given a kick change $\Delta\theta$ in BR, RSDBO at the kick location can be written as

$$\delta x_{\text{kick}} = -\Delta\theta \cdot \frac{L_1 L_2}{L_1 + L_2}.$$

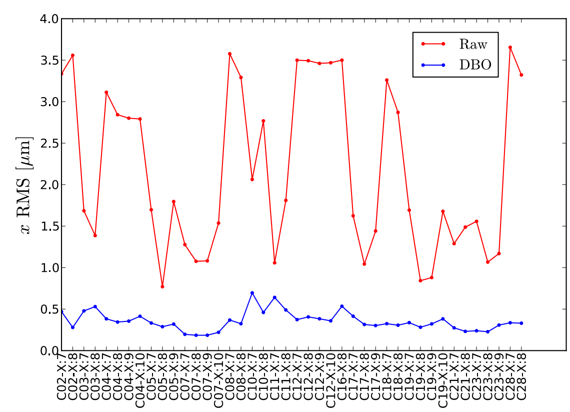

Figure 2: RMS of horizontal FA raw orbit and DBO at ID BPMs with FOFB off.

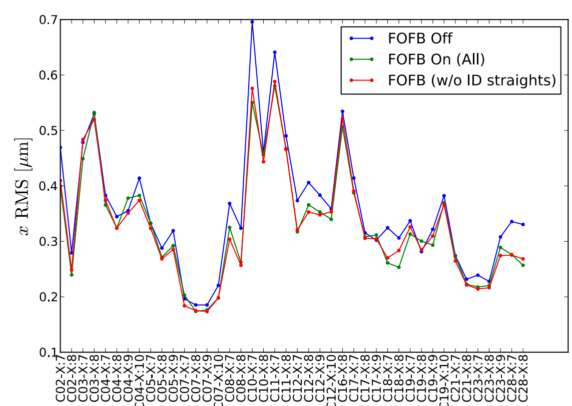

Figure 3: Comparison between FOFB off, on with and without fast correctors in BRs for RMS of horizontal FA raw orbit and DBO at ID BPMs.

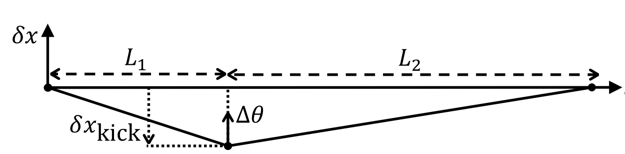

Figure 4: Relationship between a transverse kick change within BR and its effect on RSDBO.

If the total length $L_1 + L_2$ is fixed, it is obvious that $|\delta x_{\text{kick}}|$ is maximized when the kick is in the middle of BR, and approaches zero as the kick moves closer to either side of BR. Because of the relative proximity of those fast correctors to the bounding BPMs, the impact of the extra noise generated by their time-varying fast corrector kicks was

ISBN: 978-3-95450-208-0 doi:10.18429/JACoW-IPAC2019-WEPGW101

negligible. The sextupoles within BR could also corrupt RSDBO, but unless the raw orbit deviates on the order of millimeters, the kicks from the sextupoles are also negligible, which is also helped by the fact that these sextupoles are even closer to the bounding BPMs.

After the encouraging results from the RMS DBO measurements, we proceeded to generate orbit FF tables with the new method and compare them against the tables generated with the conventional method. For C05 ID, the residual orbit distortion with the FF table from either method was comparable, but the table from the new method was noticeably worse in the x-plane for the case of C12 ID.

The measured horizontal RSDBO for C12 ID was not fit well with the measured response matrix and differed significantly at C12-P8 and C12-P9 as shown in Fig. 5(a). Even though there was a potential kick difference due to non-uniformity of the dipole field by the canting magnet sitting in the middle of P8 and P9 ID BPMs, this estimated kick was too large to be true, given the very short distance between P8 and P9. The only other explanation was that these ID BPMs are physically moving when the ID gap is changed.

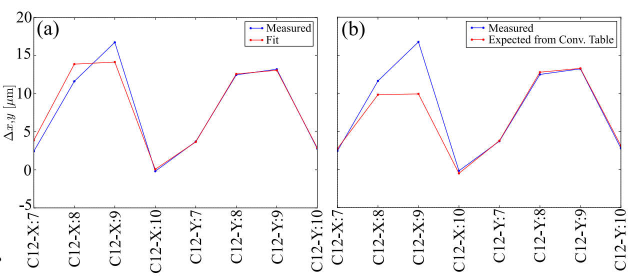

Figure 5: RSDBO for C12 ID at 6.2 mm gap. (a) Measured vs. best fit from the response matrix. (b) Measured vs. expected RSDBO from the conventional FF table.

This hypothesis is also supported by Fig. 5(b). The conventional table was separately verified to compensate well the global orbit distortion by observing at all the regular BPMs around the ring with FOFB off. Then the red curve in Fig. 5(b), the RSDBO expected from this conventional FF table and the measured response matrix using Eq. (3), should be close to the blue curve, the measured RSDBO, if ID BPMs are ideal and not moving. In other words, the large discrepancy for horizontal P8 and P9 corresponds to the ID BPM motion with the ID gap. This estimated ID BPM motion at each gap is summarized in Fig. 6, showing as much as 7 um horizontal motion, and almost no vertical motion.

This suspected ID BPM motion was later confirmed independently with direct measurements of the ID BPM buttons. Using a Keyence CL-P030 Confocal Displacement sensor, the C12 ID gap motion from the fully open state (25 mm) to 6.5 mm showed up to 8 um horizontal displacement of the P9 BPM buttons due to the connected vacuum chamber motion of 12 um. On the other hand, C05 ID gap motion moved the neighboring BPMs by no more than 2 um in both planes, measured by a TESA TT10 mechanical gauge.

It turned out that many other ID BPMs are apparently moving with the gap motions of their neighboring IDs. The worst case is observed at C17 with 30 um horizontal motion estimated from RSDBO. Due to this unexpected data corruption from ID BPM motion, a direct comparison of orbit FF tables generated from the conventional and new methods is shown only for the best case for C07 ID with <1 um BPM motion in Fig. 7. The agreement between the two methods is quite reasonable. This proves the basic principle for the new method, as long as the mechanical fix is implemented to reduce the physical BPM button motion with ID state changes.

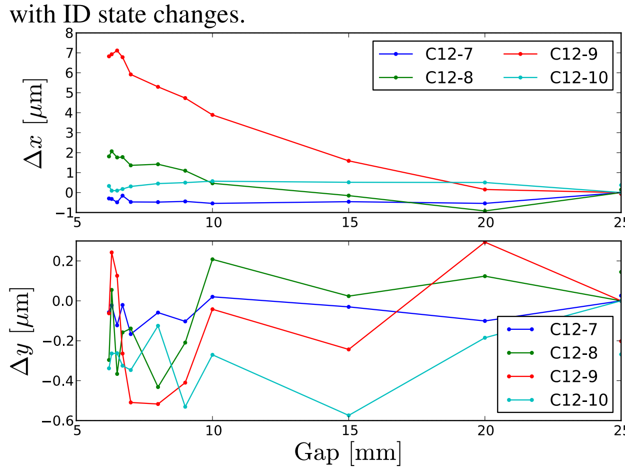

Figure 6: Estimated ID BPM physical motion with C12 ID gap motion.

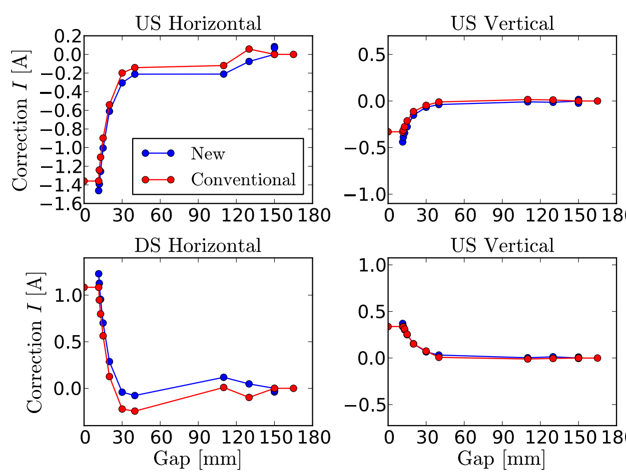

Figure 7: Orbit FF table comparison for C07 ID between the conventional and new method.

CONCLUSION

A novel method of ID orbit feedforward table generation is proposed in this paper. A unique characteristic of the newly defined dynamic orbit allows isolation of different ID straight sections during the measurement. This isolation removes the two limitations of the conventional FF table generation method, enabling simultaneous table generation for multiple IDs as well as table generation for an ID when the ID is not being utilized by the beamline scientists during a user operation period. Both lead to more time reserved for dedicated beam studies on advanced accelerator physics topics, by saving time for routine operation tasks.

ISBN: 978-3-95450-208-0 doi:10.18429/JACoW-IPAC2019-WEPGW101

REFERENCES

[1] J. Chrin, T. Schmidt, A. Streun, D. Zimoch, "Local correction schemes to counteract insertion device effects", *Nucl. Instrum. Methods Phys. Res. A*, vol 592, p. 141, 2008.

[2] Y. Hidaka *et al.,* "Investigation on Mysterious Long-Term Orbit Drift at NSLS-II," presented at IPAC'19, Melbourne, Australia, May 2019, paper WEPGW102.